Author Manuscript

Author Manuscript

Author Manuscript

Author Manuscript

HHS Public Access

Author manuscript

J Phys Chem C Nanomater Interfaces. Author manuscript; available in PMC 2021 December 17.

Published in final edited form as:

J Phys Chem C Nanomater Interfaces. 2020 December 17; 124(50): 27267–27275. doi:10.1021/acs.jpcc.0c08337.

From SERS to TERS and Beyond: Molecules as Probes of Nanoscopic Optical Fields

Patrick Z. El-Khoury[1], **Zachary D. Schultz**[2]

[1]Physical Sciences Division, Pacific Northwest National Laboratory, P.O. Box 999, Richland, WA 99352, USA

[2]Department of Chemistry and Biochemistry, The Ohio State University, Columbus, OH 43210, USA

Abstract

A detailed understanding of the interaction between molecules and plasmonic nanostructures is important for several exciting developments in (bio)molecular sensing and imaging, catalysis, as well as energy conversion. While much of the focus has been on the nanostructures that generate enhanced and nano-confined optical fields, we herein highlight recent work from our groups that uses the molecular response in surface and tip enhanced Raman scattering (SERS and TERS, respectively) to investigate different aspects of the local fields. TERS provides access to ultra-confined volumes, and as a result can further explore and explain ensemble-averaged SERS measurements. Exciting and distinct molecular behaviors are observed in the quantum limit of plasmons, including molecular charging, chemical conversion, and optical rectification. Evidence of multipolar Raman scattering from molecules additionally provides insights into the inhomogeneous electric fields that drive SERS and TERS and their spatial and temporal gradients. The time scales of these processes show evidence of cooperative nanoscale phenomena that altogether contribute to SERS and TERS.

Graphical Abstract

patrick.elkhoury@pnnl.gov.

Author Manuscript
Author Manuscript
Author Manuscript
Author Manuscript

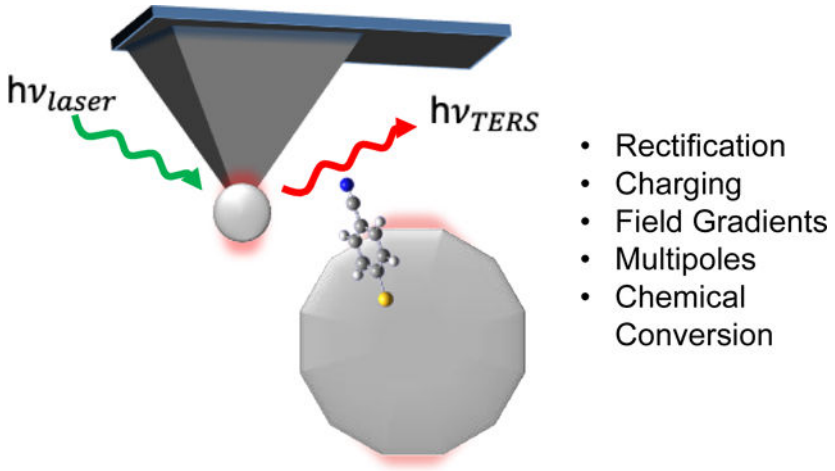

Introduction

Since the initial discovery of electromagnetic field enhancement on nanostructured metals, nanophotonics has emerged as a diverse and exciting cross-cutting field.[1–3] Photo-driven collective oscillations of surface electrons have been used to revolutionize (bio)chemical sensing, enabling ultrasensitive detection and chemical imaging with ultrahigh spatial resolution.[3] The ability to tune the plasmonic response of nanomaterials has been amply used to increase the light gathering efficiency of solar cells.[4] Additionally the relaxation of plasmons to generate energetic charge carriers has led to new approaches to photocatalyzed chemical transformations.[5] To a large extent, the focus of research has been on the nanoparticles and their properties that drive the aforementioned applications and many more.

As cross-disciplinary applications have emerged, increased understanding of plasmonic nanostructures, molecules, and their interactions have ensued. It was shown that the modes associated with plasmon resonances are governed by the shape, spacing, and organization of nanoparticles.[6] Coupling between nanoparticles was explained by plasmon hybridization theory.[7] Modeling of these interactions advanced from predominantly classical treatments to include quantum effects, which become important when particles are close enough for electrons to tunnel across junctions formed between them.[8]

The mechanisms by which plasmons relax can lead to different interfacial physical and chemical phenomena, including optical signal enhancement, heating, and hot electron generation.[9–12] An interesting observation is that when excited electrons tunnel between plasmonic structures separated by small nanometer-sized gaps, they generate direct current (DC) electric fields across the nanojunctions.[13–15] This process is known as optical rectification, in which an alternating current electric field (i.e. a plasmon) is rectified to a DC electric field at the interface.[16] It was initially observed that exciting a gap junction plasmon under bias would drive a current.[13] Later it was observed that the bias, resulting from the rectification process induced Stark shifts in molecules on the plasmonic particles.[14, 17] In these later reports, the resulting bias on the nanoparticle surface was detected using changes in the vibrational spectra of molecules *via* surface enhanced Raman scattering (SERS).

Author Manuscript Author Manuscript Author Manuscript Author Manuscript

SERS from a molecule near a plasmonic nanostructure was correlated to enhanced electric fields associated with exciting localized plasmon resonances.[3] SERS was initially largely achieved using high-density arrays of nanostructures that increase the likelihood of a molecule residing in an intense electric field region (hotspot) of the substrate. Correlations between plasmon modes and nanoparticle structures suggest that a small junction between nanoparticles gives rise to the highest enhancement, leading to the extensive use of nanoparticle aggregates[18] and nanoparticles on mirrors (NPoMs)[19] for efficient signal generation. The NPOM geometry is highly reminiscent of the tip enhanced Raman scattering (TERS) geometry, whereby a plasmonic probe is instead used to interrogate molecules and/or ultrathin material systems on metallic, but also on dielectric substrates.[20] Indeed, many high resolution and single molecule TERS measurements utilize a “gap mode” configuration, were the operative local optical fields are defined by the plasmonic tip and a metallic surface.

TERS is a powerful technique that affords both the high spatial resolution of scanning probe microscopy and the rich information content of (surface-enhanced) Raman scattering. Clean TERS measurements that take advantage of the stability of ultrahigh vacuum (UHV) and ultralow temperatures (ULT) have yielded sub-molecular spatial resolution in hyperspectral chemical nano-imaging. Indeed, even vibrational modes can be visualized in real space through UHV/ULT TERS, as elegantly illustrated by Apkarian and co-workers in a recent Nature article.[21] The increasing need for *in situ/operando* nanoscale chemical characterization and imaging led numerous TERS practitioners down the ambient nanoscopy and nano-imaging paths. Notable early efforts in this direction are summarized in prior review articles.[22–24] More recent applications that demonstrate the ever-growing potential of ambient TERS include, e.g., chemical reaction imaging at solid-liquid interfaces and nanoscale chemical mapping of single-stranded DNA with single base resolution.[25–27] Notwithstanding the ambient TERS ‘promise’ to revolutionize fields as diverse as biological imaging and plasmon-induced/enhanced (photo)chemistry, it is important to recognize that there’s much more to this technique than mere chemical identification and nano-imaging. Our ensuing discussion explores the latter by highlighting underappreciated aspects of TERS, with emphasis on what can be learned about local optical fields from molecular TERS.

In both SERS an TERS, the optical response is nascent from molecules in the vicinity of plasmonic nanostructures. Distance dependent measurements show a very short-range interaction and corroborate the latter.[28] It has been shown that the electromagnetic fields at the surface are dominated by the normal (or z-component),[29] which forms the basis for SERS and TERS selection rules that are distinct from ensemble-average Raman scattering. In many ways, this allows us to use molecules as nanoscopic probes of local optical fields, which becomes particularly powerful in single molecule SERS and TERS. In addition to the spectral response, TERS also offers the additional advantage of imaging the optical response. Through this perspective, we highlight how the molecular signals captured through SERS and TERS can provide insights into different aspects of plasmon-enhanced local optical fields.

Author Manuscript Author Manuscript Author Manuscript Author Manuscript

Discussion

Stark Shifts and Optical Rectification

The observation of large Stark shifts on plasmonic materials has generated new interest in understanding plasmonic decay channels. Stark shifts have been observed from CN[17] and CO,[14] but also from a number of CN containing compounds including mercaptobenzonitrile (MBN),[30–31] also referred to in the literature as thiobenzonitrile (TBN).[32] It was noted that SERS signals mapped on heterogeneous plasmonic arrays correlated well with Stark shifts observed from reporter molecules.[17] Vibrational Stark shifts are attributed to a change in the eigenvalue associated with a vibrational mode in a DC electric field.[33] The electric field associated with SERS and TERS is an AC field, where the incident field E_0, is enhanced on the nanoparticle and also re-radiates the scattered photons from nearby molecules, giving rise to the commonly noted E^4 scaling factor.[34] It has also been shown that intense E-fields, typically derived from pulsed lasers, can drive higher order optical processes. Indeed, optical rectification is a non-linear process deriving the from second order nonlinear optical susceptibility term, $\chi^{(2)}$. These second order processes typically require a lack of inversion symmetry, making them powerful techniques for studying surface effects and electric fields surrounding thin films.[35–36] These second order processes involve the coherent mixing of two oscillating electric fields, of doubling of single incident field. The unique relationship between optical rectification and SHG (a second order optical process) is seen through the expansion of the second order polarizability, Equation 1, which consists of the multiplication of a second order susceptibility term ($\chi^{(2)}$) and the two-alternating incident electric fields. Through expansion of this equation, terms are observed depending on two times the incident frequency (SHG) and a frequency independent term (optical rectification), Equation 3.[37]

$$P_{2NL} = X^{(2)}_{ijk} * E_i * E_j; E_i = \varepsilon_i * e^{-i\omega t} \quad [1]$$

$$= X^{(2)}_{ijk}\left[\left(\varepsilon_i * e^{-i\omega t} + \varepsilon_i^* * e^{i\omega t}\right)\left(\varepsilon_j * e^{-i\omega t} + \varepsilon_j^* * e^{i\omega t}\right)\right] \quad [2]$$

$$= X^{(2)}_{ijk}\left(\varepsilon_i\varepsilon_j e^{-2i\omega t} + \varepsilon_i\varepsilon_j^* + \varepsilon_i^*\varepsilon_j + \varepsilon_i^*\varepsilon_j^* e^{2i\omega t}\right) \quad [3]$$

Others have used this relationship to explore electric field dependencies on the optical processes;[38–39] however, the plasmon induced electric fields also drive the electric field observed on plasmonic surfaces. Indeed, plasmonic excitation has shown significant changes in surface potential, as much as −400 mV, as measured by the SHG response.[40]

Figure 1 illustrates how MBN can be used to detect the optically rectified surface potential in a SERS experiment. A plasmonic surface is functionalized with a Stark reporter molecule, such as MBN. Exciting the plasmon resonance results in a surface potential that generates a measurable Stark shift in the MBN CN stretch. Increasing the illumination intensity, as well as exciting on resonance with the plasmon frequency, results in a larger change in surface potential as measured by the Stark shift CN stretch. This is consistent with Equation 1, where stronger electric fields are expected to drive a larger rectified field. The magnitude of

Author Manuscript Author Manuscript Author Manuscript Author Manuscript

the surface potential can be calibrated using electrochemical experiments (Figure 1D), where the CN stretch frequency dependence on the surface potential can be manipulated with electrochemical control.

Correlating the Stark shifts to electron tunneling in the quantum regime has been a key insight into the origin of the observed DC fields that drive the Stark effect.[15] Classically, optical rectification is associated with materials that have directional dependent electron transport, consistent with the lack of inversion symmetry for second order optical processes. Using a NPoM configuration, the onset of Stark shifts was shown to correlate with the shift in the plasmon resonance that is associated with the quantum regime in plasmonics. In this work, computational models were used to model how small shifts in the CN Stark reporter frequency correlated to the rectified electric field, but also how electron capture, or charging, of the Stark reporter would more dramatically alter the CN stretch frequency. Recently, TERS measurements along with ab initio molecular dynamics demonstrated the same effects are observed with sub-10 nm spatial resolution.[32, 41] The presence of a TBN-anion was observed at ~ 2136 cm^{-1} in both the NPoM and TERS measurements, with a Stark shift observed near 2226 cm^{-1}, as is observed in the powder spectrum of TBN.

The sign of the rectified electric field arises from the direction of electron tunneling and can be determined from the Stark shift and tuning rate. The change in the vibrational frequency can be related to the orientation of the Stark reporter in a directional electric field. Ensemble SERS measurements of MBN show that the frequency shift can be both positive and negative of the 2226 cm^{-1} frequency of the powder. Plotting the SERS intensities of MBN vs the observed CN stretch frequency shows a minimum near 2226 cm^{-1}, suggesting a minimum in the electric field or the absence of a surface potential.[30] TERS measurement on MBN functionalized arrays also showed Stark shifts suggesting positive and negative electric fields.[41] The direction of the field remains an interesting question; however, the recent TERS work suggests changes in the coupling between the TERS tip and the plasmonic structure affects the sign of the rectified electric field. This observation is interesting in the context of prior work suggesting photo induced surface charges on plasmonic particles could be controlled by exciting the plasmon with an excitation laser either to the blue or red of the peak resonance.[42] Indeed, the position of the TERS tip relative to a nanostructure could affect the hybrid tip-substrate plasmon resonance frequency, and hence, alter the sign of the rectified field.

Beyond Stark shifts observed from molecules adsorbed to plasmonic structures, there is additional evidence of the plasmon associated rectified fields. As noted earlier, SHG measurements, performed in the absence of Stark reporters, show the same change in surface potential upon excitation of the plasmon resonance.[40] Calculations report that a femtosecond pulsed laser can excite electrons to tunnel across a nanometer sized gap on a femtosecond time scale, thereby inducing an electric field across the gap. In these calculations, the gap resides between two parallel 10 nm diameter gold nanorods.[43] However, the field induced from the single femtosecond pulse only lasts for a single optical cycle of a few fs. Previous results in our lab suggest that DC surface charge increases for as much as 10’s to 100’s of seconds under CW illumination, a clearly different time scale than a fs laser pulse.[44] While calculations show that electron tunneling occurs within femtoseconds of initial excitation;

Author Manuscript Author Manuscript Author Manuscript Author Manuscript

[43, 45] suggesting that OR and SHG do act on the same timescales initially, OR can be continuously pumped with CW illumination to produce a larger effect.[46] This longer time scale effect gives rise to the DC bias that then modulates the SHG signal. Essentially, the CW illumination provides a continuous driving force, preventing the tunneling current from reversing while illuminated. Recently, this idea of a continuous driving force was demonstrated with mechanical perturbation.[47] TERS experiments using tapping mode AFM, where the tip surface junction resides in the quantum region for approximately 10% of the experiment does not exhibit evidence of a rectified field, while Stark shifts were clearly evident from contact mode experiments where the tip remains in contact with the Au nanoplate surface.[47] The similarity in response of the rectified field to time-dependent, pulsed vs CW excitation, and mechanical perturbation, tapping vs contact mode AFM, provide discrete methods to evaluate the role of quantum plasmons in optical rectification and molecular charging, as gauged though SERS and TERS.

Imaging fields via molecular reporters

The concept of using isolated molecules as nanoscopic probes of their immediate local environments is one of the major motivations that led to the rise of single molecule microscopy and spectroscopy.[48] Naturally, the other motivation is the forward problem that is aimed at achieving the ultimate detection limit of a single molecule. However, establishing single molecule detection sensitivity, which is most straightforward in measurements performed under extreme conditions of temperature and pressure, is not necessarily a strict requirement for exploring the inverse problem. Single molecule detection is nonetheless still desirable, particularly in the context of ambient SERS and TERS. For instance, early SERS work from the Apkarian group explored the concept of 3D mapping of time varying molecular orientations by taking advantage of the tensorial nature of single molecule Raman scattering.[14] The prior work did not rigorously establish single molecule detection using one of the accepted frequency domain (e.g., the isotopologue method) or real space (e.g. atomically resolved scanning probe microscopy) proofs. Nonetheless, spectral matches between experiment and calculated tensorial Raman scattering from and oriented molecule, in combination with the prevalence of spectral diffusion and blinking established that a single molecule governed the recorded Raman spectra. In this context, the reverse problem would then be taking advantage of the tensorial nature of single molecule Raman scattering to infer the vector components of the local optical fields in its immediate vicinity. The concept is particularly powerful in the TERS scheme, as no other technique can be used to image the vector components of local optical fields with nanometer spatial resolution.

Even though ambient TERS measurements cannot resolve the inner workings of a single molecule, lateral spatial resolutions on the order of a 1–3 nm have been repeatedly demonstrated by many groups.[27, 49–51] When the tip is in contact with the substrate (more on this below), the optical signal originates from a 2D area with a diameter of 1-few nanometers. In the monolayer-sub-monolayer coverage regimes, it is then reasonable to assume that the signal arises from 1 (or very few) molecules. Overall, it important to appreciate the parallels between ultrasensitive and single molecule SERS on one hand and high spatial resolution TERS on the other. Indeed, we often need to invoke nonergodicity and/or tensorial Raman scattering to understand some of the observables in high spatial

Author Manuscript Author Manuscript Author Manuscript Author Manuscript

resolution TERS spectroscopy and imaging.[14, 52] One of our formalisms resembles the one described in Apkarian's pioneering SERS work, with one important extension: the response is spatially resolved.[53] We can therefore test the reproducibility of our measurements and explore the mechanisms behind their irreproducibility through TERS spectral imaging of symmetric and/or structurally redundant plasmonic constructs that sustain fields we can simulate exactly using finite-difference time-domain (FDTD) simulations. In a nutshell, this is the concept behind imaging the vector components of local optical fields *via* TERS, which were demonstrated using a chemically functionalized Au probe interrogating inter-terrace step-edges on Au(111).[53] In effect, the hybrid FDTD-density functional theory simulations previously reported may be used to forward simulate both ultrasensitive and ensemble-averaged TERS spectral images.

Increasing the number of molecules and/or increasing the effective TERS probing volume reduces the dimensionality and complexity of the problem. Mathematically, this involves averaging over molecular orientation in measurements governed by TERS selection rules: incident/scattered radiation is preferentially enhanced along the tip axis, which is orthogonal to the sample surface (along the z-direction). In this case, we found that TERS images of various chemically functionalized plasmonic nanostructures broadcast the z-components of the local optical fields in their immediate vicinities, see Figure 2. Although the latter can be ascertained through FDTD simulations of some structures, e.g., nanocubes (2A) and smooth spherical nanoparticles (2C), other TERS images cannot be readily rationalized. For instance, the scattering pattern observed from faceted silver nanoparticles (2B) is very dissimilar from spherical particles (2C). The scattering pattern traces the facet boundaries that are characteristic of the former nanostructures. Indeed, the correspondence between simultaneously recorded AFM and TERS images, polarization-resolved TERS mapping, as well as the contrast with nanocubes and spherical nanoparticles together support the proposed picture and assignment. The TERS images of Au nanorods (2D) are again unique. In the plot shown herein (Figure 2D), the TERS map traces the z-component of the multipolar (m=3) longitudinal plasmonic mode of the rod. More generally, both dipolar and multipolar resonances of these nanostructures can be imaged *via* TERS. In effect, and within the same hyperspectral TERS image cube, sequential transitions between high-order modes at low frequency shifts and lower-order modes at higher frequencies were observed.[54] This nanorod work thus adds a new dimension to local optical field mapping via TERS: not only can the vector components and spatial profiles of local optical fields be imaged; spatially varying local optical resonances are direct observables. This recent realization may hold the key to understanding the TERS maps of corrugated surfaces and nanostructures, where local resonances have been found to span the deep-UV through mid-IR spectral region.[55] Note that all the aforementioned AFM-based TERS measurements were recorded using corrugated/sputtered probes with an intermittent contact mode feedback, whereby the tip is in contact when the spectra are measured and in semi-contact as the sample is scanned relative to the probe. As noted above, the proximity of the tip to the surface appears to modulate the accessed plasmon and the electric field environment. Further, the nanostructures were otherwise functionalized with the same molecular reporter (MBN).

Throughout the course of TERS mapping of chemically functionalized plasmonic nanoparticles, only a few of which are shown in Figure 2, we noticed that the extent of local

Author Manuscript Author Manuscript Author Manuscript Author Manuscript

optical field confinement (or the plasmonic nanoparticles themselves) governs the measured/apparent spatial resolution. For instance, ultra-confined signals towards the edges of silver nanocubes (< 2nm) are contrasted with less confined (~10–15 nm) fields along the edges of crystalline gold nanoplatelets. Both can be rationalized on the basis of FDTD simulations of the two nanostructures (without including the probe). There are several interesting aspects to this observation. First, we recently rigorously illustrated that the field-limited/apparent spatial resolution is coarser than the actual spatial resolution that is attainable in ambient TERS.[56] The case was made using two different analytes that are chemisorbed onto plasmonic gold nanoplates. We were able to distinguish between the two molecules on a length scale that is much finer than the spread in the profile of the local optical field, which we often rely on to infer the spatial resolution in our measurements. The second aspect of this observation has to do with the nature of the interaction between the probe and the nanostructures. Our current understanding is that molecular TERS simply reports on fields that are sustained near the different nanostructures and nanoparticles we probe. In other words, a clean TERS probe merely reveals/reads out the optical fields that are sustained at the surface of the nanoparticle. This becomes somewhat evident when the recorded images (e.g., in Figure 2) are compared to FDTD simulations of the local optical fields of the different structures. The next question then has to do with the nature of the interaction between the molecular probe and plasmonic nanoparticles.

Optical Charging and Chemical Conversion vs Multipolar Raman

Thus far, we have established a basis for using molecules to inform about electric fields based largely on the assumption that the molecules and plasmonic metals can be treated separately. In this section we point out clear examples where changes in the observed spectrum arise from plasmon-induced physical and chemical changes in the reporter molecule. As noted earlier, the excitation of plasmon resonances can drive currents between nanostructures, giving rise to rectified fields. However, the electron does not always travel across the junction to a particle. The transition from classical field enhancing junction plasmons to charge shuttling quantum plasmons led to numerous interesting demonstrations and to an enhanced understanding of some of the observables in Raman spectroscopy at plasmonic nanojunctions. A classic example was the demonstration that dimercaptoazobenzene (DMAB) can be formed as a photoproduct from aminothiophenol on plasmonic surfaces.[57–58] Increasing evidence suggests the electron can also become trapped on molecules in the junction, giving rise to molecular signatures derived from anion, or radical, forms of the molecule. As mentioned above, subtle shifts attributed to Stark shifts in the nominal (~2225 cm^{-1}) resonance frequency of the aromatic nitrile stretching vibrational mode are indicative of rectified local optical fields. More extreme shifts (~−100 cm^{-1}) in the same spectral region can be rigorously assigned to molecular charging (Figure 3A).

Molecular charging in plasmonic nanogaps has been observed in other systems as well, suggesting a more common molecular behavior that has not been fully appreciated. In addition to MBN, evidence of an anion like species has also been observed for nitrothiophenol (NTP),[59–60] polymethine dyes,[61] and recently for tryptophan residues in proteins.[62] In NTP, DFT calculations were matched to the observed TERS spectrum to show the observed vibrational features could be readily explained by reduction of NTP molecule.

Author Manuscript Author Manuscript Author Manuscript Author Manuscript

This molecular charging correlated with formation of a quantum plasmon and was suppressed in the TERS measurement using tapping mode feedback to limit the observed quantum effects.[59] With tryptophan, the SERS spectrum observed from colloidal Au nanoparticles exhibited a Raman spectrum and electronic resonance readily explained by the radical anion species.[62] While the HOMO-LUMO gap for tryptophan lies in the ultraviolet region of the visible spectrum, radicals formed by the capture of an electron show lower energy transitions that give rise to surface enhanced *resonance* Raman scattering (SERRS). A similar rationale was presented for polymethine dyes on Ag nanoaggregates.[61] Conversely, the capture of plasmonically excited electrons has also been reported to fragment biomolecules in TERS experiments.[63]

At this point, it is important to note that multipolar Raman scattering needs to be ruled out prior to assigning new spectral features (e.g. - non-Raman active modes) to charged species and photoproducts. In the fingerprint region of the spectrum (3B) conventional (α^2, electric dipole-electric dipole) Raman scattering is observed. We have also observed and assigned tip-enhanced multipolar Raman scattering.[64] Shown in Figure 3B are theoretical and experimental enhanced electric dipole-magnetic dipole (m^2) and electric dipole-electric quadrupole (A^2) TERS. Definitive assignments were only possible because of our choice of molecular reporter and theoretical analysis: conventional (dipolar) selection rules cannot account for the peaks we observe in the 1250–1500 cm^{-1} spectral region. Overall, the observation of multipolar TERS implicates large electric field gradients that vary over typical molecular length scales in the TERS geometry. This is expected, given the corrugated nature of our AFM probes and the extreme nano-confinement of the signals, and hence, of the fields.

The molecular signals observed in SERS and TERS need to be carefully analyzed. Namely, signals from molecular reporters can provide unique physical insights and information about their immediate local environments, i.e., the local optical fields. Understanding the distinct behaviors of different molecules interacting with enhanced local fileds will be important to various applications. The prevalence and generality of molecular charging on SERS and TERS signals remains to be fully investigated. The formation of resonantly enhanced species could dominate the observed spectrum with the signal from a minority of molecules. Charging of tryptophan is observed in some proteins[62], but not in others.[65] This may be explained by the electron residing in the lowest energy conformation, which may be the indole ring but can also be a coordinated metal. Rationalizing the increase in polarizability of these molecules with their prevalence in junctions remains an intriguing question. Of further relevance, beyond enhancing signals, electron capture has also been shown to induce fragmentation[63, 66] and photoconversion[57]. Indeed, as the role of plasmonic junctions in photoconversion and catalysis becomes more appreciated,[5] it is clear that the nature of molecules at the junctions are increasingly relevant to the observed behavior. Jain and co-workers have proposed that the preferential electron transfer to molecules drives the photo-potentials observed on plasmonic particles and have developed a formalism to describe the free energy change associated with photo induced surface charging.[67–68] Here SERS and TERS measurements provide additional insight. In fact, plasmonic photoconversion rates have been shown to correlate with photopotentials.[69] Of further interest, molecular anions

Author Manuscript Author Manuscript Author Manuscript Author Manuscript

formed at plasmonic junctions show similar Stark tuning rates to the neutral molecule,[41] suggesting that charging and photo-potential may operate via independent mechanisms.

Conclusion

Here we have highlighted how molecules in plasmonic junctions can be used monitor properties of the electric field, but also how the electric fields can alter molecules in the immediate vicinity of photo-excited plasmonic metals. Besides the nature of the molecular reporter, the power of the incident laser, and the use of pulsed vs. CW laser sources, the feedback (tapping *vs* contact mode) used in TERS comprises a useful knob for selectively accessing the classical regime of bonding dipolar-type modes and the quantum realm of charge transfer plasmons. On the basis of our observations, it appears that plasmon-induced/enhanced chemical transformations may be switched on/off in quantum/classical junction plasmon-enhanced TERS. Furthermore, of importance to the topic of this perspective is the observation that only quantum plasmons are rectified in the TERS geometry.

The generality of these recent observations needs to be checked using different molecular reporters. The observed molecular response arises from the properties of the molecule and may be specific to classes of molecules rather than widely applicable to all cases. Additionally, the relative magnitude of the reported behaviors (charging, photoconversion, multipoles, etc.) need to be evaluated to aid in identifying the dominant behaviors evident in SERS and TERS spectra. It is quite possible multiple effects are observed simultaneously, contributing to the observed response.

Interestingly, quantum plasmons appear to drive molecular charging, which can result in both signal enhancement and degradation. The time scales associated with electron capture appear to be a critical element. There is evidence of both ultrafast and longer-lived processes regulated by plasmonic excitation and decay channels. The impact of plasmonic fields and resulting energetic charge carriers on nearby molecules, but also using these molecules to understand the resulting fields, appear to be equally exciting areas for future development in this field.

Acknowledgments

PZE acknowledges support from the US Department of Energy, Office of Science, Office of Basic Energy Sciences, Division of Chemical Sciences, Geosciences & Biosciences. ZDS acknowledges support from the National Institutes of Health Award R01 GM109988, a Cottrell Scholars award, a program of Research Corporation for Science Advancement, and The Ohio State University.

AUTHOR BIOGRAPHIES

Patrick El-Khoury received a B.Sc. in chemistry from the American University of Beirut (2003–2006, advisor: B. R. Kaafarani), a Ph.D. in photochemical sciences from Bowling Green State University (2006–2010, advisor: A. N. Tarnovsky), and postdoctoral training at the University of California, Irvine (2010–2012, advisor: V. A. Apkarian). Soon after, he joined Pacific Northwest National Laboratory (PNNL) as a Linus Pauling Distinguished Postdoctoral Research fellow (2013–2016, mentor: W. P. Hess). Patrick is currently a senior research scientist in the chemical physics and analysis group, within the physical sciences

Author Manuscript Author Manuscript Author Manuscript Author Manuscript

division at PNNL. Among other things, he spends his days worrying about molecules, plasmons, and their interactions as gauged through tip-enhanced Raman nano-spectroscopy and nano-imaging.

Zachary Schultz is an associate professor of chemistry and biochemistry at the Ohio State University. He obtained his B.S. majoring in chemistry from The Ohio State University in 2000, Ph.D. from the University of Illinois at Urbana-Champaign in 2005, and postdoctoral training the National Institute of Standards and Technology and National Institute for Diabetes and Digestive and Kidney Diseases. He began his independent career as an assistant professor at the University of Notre Dame in 2009 and moved his laboratory to the Ohio State University in 2018. His research interests include understanding light – molecule – nanoparticle interactions and their application for (bio)chemical detection and imaging.

El Khoury

Schultz

References:

1. Jeanmaire DL; Van Duyne RP, Surface Raman Spectroelectrochemistry: Part I. Heterocyclic, Aromatic, and Aliphatic Amines Adsorbed on the Anodized Silver Electrode. Journal of Electroanalytical Chemistry and Interfacial Electrochemistry 1977, 84, 1–20.
2. Moskovits M, Surface Roughness and the Enhanced Intensity of Raman Scattering by Molecules Adsorbed on Metals. The Journal of Chemical Physics 1978, 69, 4159–4161.
3. Langer J; Jimenez de Aberasturi D; Aizpurua J; Alvarez-Puebla RA; Auguié B; Baumberg JJ; Bazan GC; Bell SEJ; Boisen A; Brolo AG, et al., Present and Future of Surface Enhanced Raman Scattering. ACS Nano 2019, 14, 28–117. [PubMed: 31478375]
4. Jang YH; Jang YJ; Kim S; Quan LN; Chung K; Kim DH, Plasmonic Solar Cells: From Rational Design to Mechanism Overview. Chem Rev 2016, 116, 14982–15034. [PubMed: 28027647]
5. Zhang YC; He S; Guo WX; Hu Y; Huang JW; Mulcahy JR; Wei WD, Surface-Plasmon-Driven Hot Electron Photochemistry. Chem. Rev 2018, 118, 2927–2954. [PubMed: 29190069]
6. Halas NJ; Lal S; Chang WS; Link S; Nordlander P, Plasmons in Strongly Coupled Metallic Nanostructures. Chem. Rev 2011, 111, 3913–3961. [PubMed: 21542636]
7. Prodan E; Radloff C; Halas NJ; Nordlander P, A Hybridization Model for the Plasmon Response of Complex Nanostructures. Science 2003, 302, 419–422. [PubMed: 14564001]
8. Savage KJ; Hawkeye MM; Esteban R; Borisov AG; Aizpurua J; Baumberg JJ, Revealing the Quantum Regime in Tunnelling Plasmonics. Nature 2012, 491, 574–577. [PubMed: 23135399]
9. Linic S; Christopher P; Ingram DB, Plasmonic-Metal Nanostructures for Efficient Conversion of Solar to Chemical Energy. Nat Mater 2011, 10, 911–921. [PubMed: 22109608]

Author Manuscript Author Manuscript Author Manuscript Author Manuscript

10. Jain PK; Huang X; El-Sayed IH; El-Sayed MA, Noble Metals on the Nanoscale: Optical and Photothermal Properties and Some Applications in Imaging, Sensing, Biology, and Medicine. Accounts of Chemical Research 2008, 41, 1578–1586. [PubMed: 18447366]
11. Brus L, Noble Metal Nanocrystals: Plasmon Electron Transfer Photochemistry and Single-Molecule Raman Spectroscopy. Accounts of Chemical Research 2008, 41, 1742–1749. [PubMed: 18783255]
12. Chen X; Zheng Z; Ke X; Jaatinen E; Xie T; Wang D; Guo C; Zhao J; Zhu H, Supported Silver Nanoparticles as Photocatalysts under Ultraviolet and Visible Light Irradiation. Green Chemistry 2010, 12, 414–419.
13. Ward DR; Huser F; Pauly F; Cuevas JC; Natelson D, Optical Rectification and Field Enhancement in a Plasmonic Nanogap. Nat Nano 2010, 5, 732–736.
14. Banik M; El-Khoury PZ; Nag A; Rodriguez-Perez A; Guarrottxena N; Bazan GC; Apkarian VA, Surface-Enhanced Raman Trajectories on a Nano-Dumbbell: Transition from Field to Charge Transfer Plasmons as the Spheres Fuse. ACS Nano 2012, 6, 10343–10354. [PubMed: 23092179]
15. Wang H; Yao K; Parkhill JA; Schultz ZD, Detection of Electron Tunneling across Plasmonic Nanoparticle-Film Junctions Using Nitrile Vibrations. Physical Chemistry Chemical Physics 2017, 19, 5786–5796. [PubMed: 28180214]
16. Shen YR, The Principles of Nonlinear Optics; J. Wiley: New York, 1984.
17. Marr JM; Schultz ZD, Imaging Electric Fields in Sers and Ters Using the Vibrational Stark Effect. The Journal of Physical Chemistry Letters 2013, 4, 3268–3272.
18. Wustholz KL; Henry A-I; McMahon JM; Freeman RG; Valley N; Piotti ME; Natan MJ; Schatz GC; Van Duyne RP, Structure-Activity Relationships in Gold Nanoparticle Dimers and Trimers for Surface-Enhanced Raman Spectroscopy. J. Am. Chem. Soc 2010, 132, 10903–10910. [PubMed: 20681724]
19. Carnegie C; Griffiths J; de Nijs B; Readman C; Chikkaraddy R; Deacon WM; Zhang Y; Szabó I; Rosta E; Aizpurua J, et al., Room-Temperature Optical Picocavities Below 1 Nm3 Accessing Single-Atom Geometries. The Journal of Physical Chemistry Letters 2018, 9, 7146–7151. [PubMed: 30525662]
20. Zhang R; Zhang Y; Dong ZC; Jiang S; Zhang C; Chen LG; Zhang L; Liao Y; Aizpurua J; Luo Y, et al., Chemical Mapping of a Single Molecule by Plasmon-Enhanced Raman Scattering. Nature 2013, 498, 82–86. [PubMed: 23739426]
21. Lee J; Crampton KT; Tallarida N; Apkarian VA, Visualizing Vibrational Normal Modes of a Single Molecule with Atomically Confined Light. Nature 2019, 568, 78–82. [PubMed: 30944493]
22. Kurouski D; Dazzi A; Zenobi R; Centrone A, Infrared and Raman Chemical Imaging and Spectroscopy at the Nanoscale. Chemical Society Reviews 2020, 49, 3315–3347.
23. Zrimsek AB; Chiang NH; Mattei M; Zaleski S; McAnally MO; Chapman CT; Henry AI; Schatz GC; Van Duyne RP, Single-Molecule Chemistry with Surface- and Tip-Enhanced Raman Spectroscopy. Chem. Rev 2017, 117, 7583–7613. [PubMed: 28610424]
24. Deckert-Gaudig T; Taguchi A; Kawata S; Deckert V, Tip-Enhanced Raman Spectroscopy - from Early Developments to Recent Advances. Chemical Society Reviews 2017, 46, 4077–4110. [PubMed: 28640306]
25. Wang X; Huang SC; Huang TX; Su HS; Zhong JH; Zeng ZC; Li MH; Ren B, Tip-Enhanced Raman Spectroscopy for Surfaces and Interfaces. Chemical Society Reviews 2017, 46, 4020–4041. [PubMed: 28590479]
26. Zeng Z-C; Huang S-C; Wu D-Y; Meng L-Y; Li M-H; Huang T-X; Zhong J-H; Wang X; Yang Z-L; Ren B, Electrochemical Tip-Enhanced Raman Spectroscopy. J. Am. Chem. Soc 2015, 137, 11928–11931. [PubMed: 26351986]
27. He Z; Han Z; Kizer M; Linhardt RJ; Wang X; Sinyukov AM; Wang J; Deckert V; Sokolov AV; Hu J, et al., Tip-Enhanced Raman Imaging of Single-Stranded DNA with Single Base Resolution. J. Am. Chem. Soc 2019, 141, 753–757. [PubMed: 30586988]
28. Asiala SM; Schultz ZD, Surface Enhanced Raman Correlation Spectroscopy of Particles in Solution. Anal. Chem 2014, 86, 2625–2632. [PubMed: 24502388]
29. Novotny L; Hecht B, Principles of Nano-Optics; Cambridge University Press: Cambridge ; New York, 2006, p xvii, 539 p.

Author Manuscript Author Manuscript Author Manuscript Author Manuscript

30. Kwasnieski DT; Wang H; Schultz ZD, Alkyl-Nitrile Adlayers as Probes of Plasmonically Induced Electric Fields. Chem Sci 2015, 6, 4484–4494. [PubMed: 26213606]
31. Oklejas V; Sjostrom C; Harris JM, Sers Detection of the Vibrational Stark Effect from Nitrile-Terminated Sams to Probe Electric Fields in the Diffuse Double-Layer. J. Am. Chem. Soc 2002, 124, 2408–2409. [PubMed: 11890768]
32. Bhattarai A; Cheng Z; Joly AG; Novikova IV; Evans JE; Schultz ZD; Jones MR; El-Khoury PZ, Tip-Enhanced Raman Nanospectroscopy of Smooth Spherical Gold Nanoparticles. The Journal of Physical Chemistry Letters 2020, 1795–1801.
33. Boxer SG, Stark Realities. J. Phys. Chem. B 2009, 113, 2972–2983. [PubMed: 19708160]
34. Kerker M, Estimation of Surface-Enhanced Raman Scattering from Surface-Averaged Electromagnetic Intensities. Journal of Colloid and Interface Science 1987, 118, 417–421.
35. W. Boyd R, Chapter 1. The Nonlinear Optical Susceptibility, 2003, p 1–65.
36. Saleh, B. T. M;, Nonlinear Optics. In Fundamentals of Photonics, Second Edition, Saleh B, Ed. Wiley Interscience: 2007.
37. Powers PE, Fundamentals of Nonlinear Optics; CRC Press, 2011.
38. Gonella G; Lütgebaucks C; de Beer AGF; Roke S, Second Harmonic and Sum-Frequency Generation from Aqueous Interfaces Is Modulated by Interference. The Journal of Physical Chemistry C 2016, 120, 9165–9173.
39. Ohno PE; Wang H.-f.; Geiger FM, Second-Order Spectral Lineshapes from Charged Interfaces. Nat. Commun 2017, 8, 1032. [PubMed: 29044095]
40. Nelson DA; Schultz ZD, Impact of Plasmon-Induced Optically Rectified Electric Fields on Second Harmonic Generation. J. Phys. Chem. C 2019, 123, 20639–20648.
41. Bhattarai A; Crampton KT; Joly AG; Wang C-F; Schultz ZD; El-Khoury PZ, A Closer Look at Corrugated Au Tips. The Journal of Physical Chemistry Letters 2020, 1915–1920.
42. Sheldon MT; van de Groep J; Brown AM; Polman A; Atwater HA, Plasmoelectric Potentials in Metal Nanostructures. Science 2014, 1258405.
43. Aguirregabiria G; Marinica D-C; Ludwig M; Brida D; Leitenstorfer A; Aizpurua J; Borisov AG, Dynamics of Electron-Emission Currents in Plasmonic Gaps Induced by Strong Fields. Faraday Discuss. 2019, 214, 147–157. [PubMed: 30834916]
44. Nelson DA; Schultz ZD, The Impact of Optically Rectified Fields on Plasmonic Electrocatalysis. Faraday Discuss 2019, 214, 465–477. [PubMed: 30821795]
45. Aguirregabiria G; Marinica DC; Esteban R; Kazansky AK; Aizpurua J; Borisov AG, Role of Electron Tunneling in the Nonlinear Response of Plasmonic Nanogaps. Phys Rev B 2018, 97, 115430.
46. Rybka T; Ludwig M; Schmalz MF; Knittel V; Brida D; Leitenstorfer A, Sub-Cycle Optical Phase Control of Nanotunnelling in the Single-Electron Regime. Nature Photonics 2016, 10, 667–670.
47. Wang C-F; O'Callahan BT; Kurouski D; Krayev AV; Schultz ZD; El-Khoury PZ, Suppressing Molecular Charging, Nano-Chemistry, and Optical Rectification in the Tip-Enhanced Raman Geometry. The Journal of Physical Chemistry Letters 2020.
48. Moerner WE, Nobel Lecture: Single-Molecule Spectroscopy, Imaging, and Photocontrol: Foundations for Super-Resolution Microscopy. Rev. Mod. Phys 2015, 87, 1183–1212.
49. El-Khoury PZ; Aprà E, Spatially Resolved Mapping of Three-Dimensional Molecular Orientations with ~2 Nm Spatial Resolution through Tip-Enhanced Raman Scattering. The Journal of Physical Chemistry C 2020, 124, 17211–17217.
50. Bhattarai A; Novikova IV; El-Khoury PZ, Tip-Enhanced Raman Nanographs of Plasmonic Silver Nanoparticles. The Journal of Physical Chemistry C 2019, 123, 27765–27769.
51. Chen C; Hayazawa N; Kawata S, A 1.7 Nm Resolution Chemical Analysis of Carbon Nanotubes by Tip-Enhanced Raman Imaging in the Ambient. Nat. Commun 2014, 5, 3312. [PubMed: 24518208]
52. Apra E; Bhattarai A; Crampton KT; Bylaska EJ; Govind N; Hess WP; El-Khoury PZ, Time Domain Simulations of Single Molecule Raman Scattering. The journal of physical chemistry. A 2018, 122, 7437–7442. [PubMed: 30148635]

Author Manuscript Author Manuscript Author Manuscript Author Manuscript

53. Bhattarai A; Joly AG; Hess WP; El-Khoury PZ, Visualizing Electric Fields at Au(111) Step Edges Via Tip-Enhanced Raman Scattering. Nano Lett 2017, 17, 7131–7137. [PubMed: 28972773]
54. Bhattarai A; O'Callahan BT; Wang C-F; Wang S; El-Khoury PZ, Spatio-Spectral Characterization of Multipolar Plasmonic Modes of Au Nanorods Via Tip-Enhanced Raman Scattering. The Journal of Physical Chemistry Letters 2020, 11, 2870–2874.
55. Abellan P; El-Khoury PZ; Ramasse QM, Mapping Vis-Terahertz (≤17 Thz) Surface Plasmons Sustained on Native and Chemically Functionalized Percolated Gold Thin Films Using Eels. Microscopy 2017, 67, i30–i39.
56. O'Callahan BT; Bhattarai A; Schultz ZD; El-Khoury PZ, Power-Dependent Dual Analyte Tip-Enhanced Raman Spectral Imaging. The Journal of Physical Chemistry C 2020, 124, 15454–15459.
57. Huang Y-F; Zhu H-P; Liu G-K; Wu D-Y; Ren B; Tian Z-Q, When the Signal Is Not from the Original Molecule to Be Detected: Chemical Transformation of Para-Aminothiophenol on Ag During the Sers Measurement. J. Am. Chem. Soc 2010, 132, 9244–9246. [PubMed: 20527877]
58. Fang Y; Li Y; Xu H; Sun M, Ascertaining P P′-Dimercaptoazobenzene Produced from P-Aminothiophenol by Selective Catalytic Coupling Reaction on Silver Nanoparticles. Langmuir 2010, 26, 7737–7746. [PubMed: 20455558]
59. Wang CF; O'Callahan BT; Kurouski D; Krayev A; Schultz ZD; El-Khoury PZ, Suppressing Molecular Charging, Nanochemistry, and Optical Rectification in the Tip-Enhanced Raman Geometry. J Phys Chem Lett 2020, 5890–5895.
60. Wang R; Li J; Rigor J; Large N; El-Khoury PZ; Rogachev AY; Kurouski D, Direct Experimental Evidence of Hot Carrier-Driven Chemical Processes in Tip-Enhanced Raman Spectroscopy (TERS). The Journal of Physical Chemistry C 2020, 124, 2238–2244.
61. Kneipp K, Chemical Contribution to Sers Enhancement: An Experimental Study on a Series of Polymethine Dyes on Silver Nanoaggregates. The Journal of Physical Chemistry C 2016, 120, 21076–21081.
62. Sloan-Dennison S; Zoltowski CM; El-Khoury PZ; Schultz ZD, Surface Enhanced Raman Scattering Selectivity in Proteins Arises from Electron Capture and Resonant Enhancement of Radical Species. The Journal of Physical Chemistry C 2020, 124, 9548–9558.
63. Szczerbiński J; Gyr L; Kaeslin J; Zenobi R, Plasmon-Driven Photocatalysis Leads to Products Known from E-Beam and X-Ray-Induced Surface Chemistry. Nano Lett 2018, 18, 6740–6749. [PubMed: 30277787]
64. Wang C-F; Cheng Z; O'Callahan BT; Crampton KT; Jones MR; El-Khoury PZ, Tip-Enhanced Multipolar Raman Scattering. The Journal of Physical Chemistry Letters 2020, 11, 2464–2469.
65. Kradolfer S; Lipiec E; Baldacchini C; Bizzarri AR; Cannistraro S; Zenobi R, Vibrational Changes Induced by Electron Transfer in Surface Bound Azurin Metalloprotein Studied by Tip-Enhanced Raman Spectroscopy and Scanning Tunneling Microscopy. ACS Nano 2017, 11, 12824–12831. [PubMed: 29202236]
66. Szczerbiński J; Metternich JB; Goubert G; Zenobi R, How Peptides Dissociate in Plasmonic Hot Spots. Small 2020, 16, 1905197.
67. Yu S; Jain PK, The Chemical Potential of Plasmonic Excitations. Angewandte Chemie 2020, 59, 2085–2088.
68. Wilson AJ; Jain PK, Light-Induced Voltages in Catalysis by Plasmonic Nanostructures. Accounts Chem. Res 2020.
69. Nelson DA; Schultz ZD, Influence of Optically Rectified Electric Fields on the Plasmonic Photocatalysis of 4-Nitrothiophenol and 4-Aminothiophenol to 4,4-Dimercaptoazobenzene. J. Phys. Chem. C 2018, 122, 8581–8588.

Author Manuscript
Author Manuscript
Author Manuscript
Author Manuscript

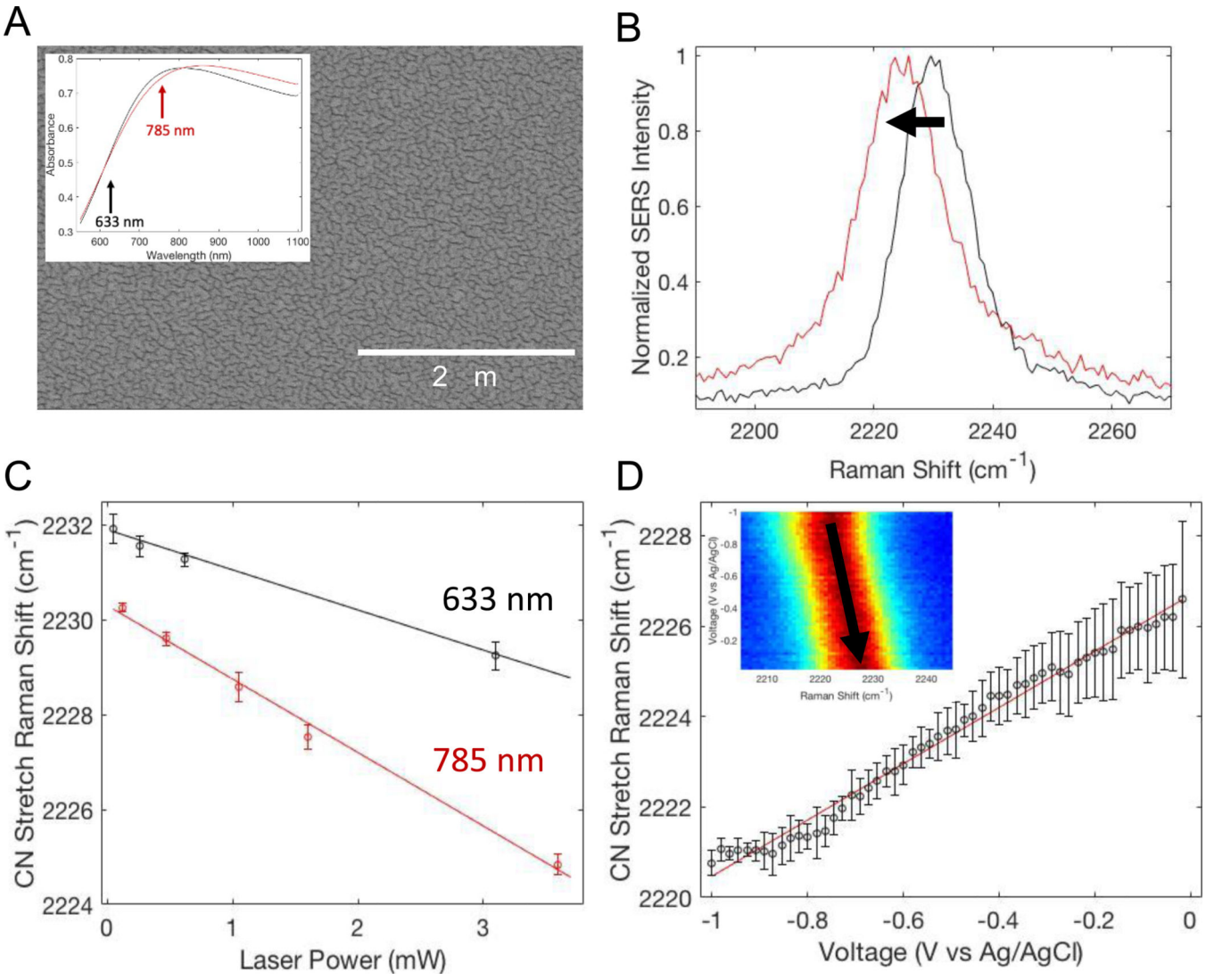

Figure 1.

depicts a gold nanoisland film SERS substrate and the detection of the optically rectified field by an adsorbed MBN molecule. A) the SEM image of the surface shows a heterogeneous arrangement of nanostructures. The inset shows a broad resonance (black) consistent with coupled plasmons. Absorption of the MBN induces a slight redshift in the observed extinction spectrum (red). B) Illuminating the SERS substrate induces a reversible shift in the CN stretch. The black spectrum was obtained at low fluence, while increased light fluence produces the red spectrum. C) The shift in frequency on the SERS substrate is shown to track with increased laser power. Illuminating on resonance produces a larger change in the observed frequency. D). The shift in CN frequency can also be induced electrochemically, where a negative surface potential correlates with a lower CN stretch frequency. The inset shows how the CN stretching mode evolves with applied electrochemical potential. Figure adapted from Ref. 40 (American Chemical Society, 2019), used with permission.

Author Manuscript Author Manuscript Author Manuscript Author Manuscript

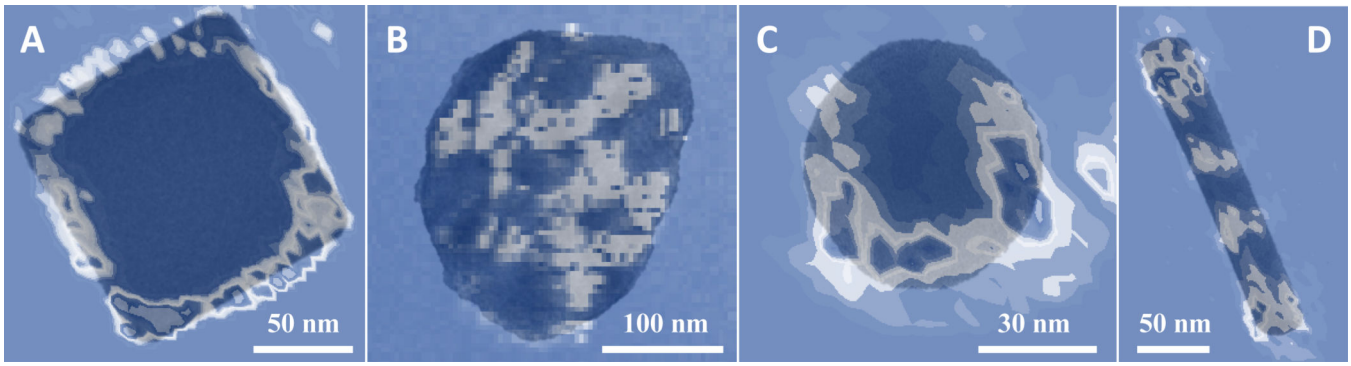

Figure 2.

TERS maps (633 nm excitation) of a plasmonic silver nanocube (A), a faceted silver nanoparticle (B), a smooth gold nanoparticle (C), and a single crystal gold nanorod (D). All of these particles are supported on a silicon substrate. The chemical images are overlaid on top of TEM images of similarly shaped nanoparticles for reference. In practice, correlated/simultaneous AFM-TERS mapping is performed to visualize both topography and chemistry in the TERS geometry.

Author Manuscript Author Manuscript Author Manuscript Author Manuscript

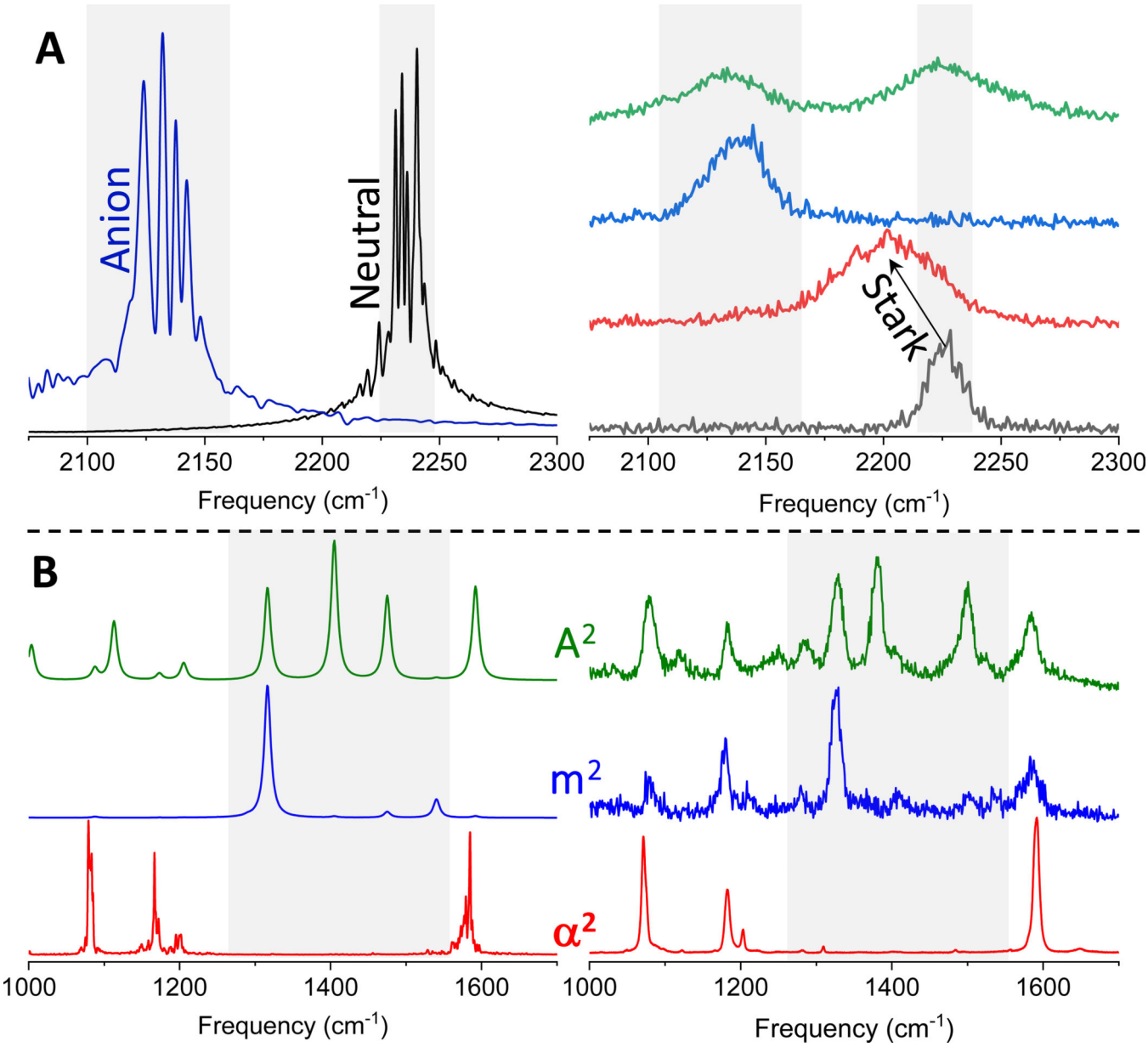

Figure 3.

A) The left panel shows theoretical ab initio molecular dynamics (AIMD)-based Raman spectral simulation of the nitrile resonances of the neutral and anionic (singly charged) TBN species. The right panel shows selected single pixel spectra, in which (bottom to top) the neutral, Stark-shifted neutral, anionic, and both parent and anionic nitrile resonances are observed. These spectra were recorded from the nanosphere shown in Figure 2A, using a sputtered Au TERS probe. B) The left panel shows theoretical enhanced electric dipole-electric dipole (α^2), electric dipole-magnetic dipole (m^2), and electric dipole electric quadrupole (A^2) TERS spectra. The conventional Raman spectrum was computed using AIMD-based Raman spectral simulations, whereas the multipolar spectra were computed through differentiation at the minimum energy geometry of TBN. Corresponding experimental spectra (selected single pixel spectra) recorded at the nanojunctions formed

between a sputtered Ag tip and a ~70 nm gold nano-cube are shown in the right panel. All of the theoretical spectra were computed at the pbe/def2-TZVP level of theory.

Author Manuscript Author Manuscript Author Manuscript Author Manuscript